EUROPEAN ORGANIZATION FOR NUCLEAR RESEARCH
ORGANISATION EUROPEENNE POUR LA RECHERCHE NUCLEAIRE

CERN - PS DIVISION

PS/ CA/ Note 98-19
AD Note036

THE MEASUREMENT LINE AT THE ANTIPROTON DECELERATOR

U. Mikkelsen
Institute for Storage Ring Facilities, ISA, University of Aarhus,
DK-8000 Aarhus C, Denmark

Geneva, Switzerland
6 August 1998

The measurement line at the Antiproton Decelerator

Ulrik Mikkelsen
Institute for Storage Ring Facilities, ISA, University of Aarhus,
DK–8000 Aarhus C, Denmark
and
PS-CA, CERN,
CH-1211 Geneva 23, Switzerland
E-mail: ulrik@dfi.aau.dk, ulrik.mikkelsen@cern.ch

July 27, 1998

Abstract

The optics and basic parameters for the so-called measurement line at the Antiproton Decelerator (AD) are described. This line is intended to serve several purposes and thus a number of different optics are studied. First, the line must provide measurements of important parameters of the AD beam such as the emittance and momentum spread. Second, it must be able to serve as a test beam for the Radio Frequency Quadrupole (RFQ) to be installed in the DE1 line. Third, a parallel beam must be available for studies of antiproton channeling and finally there must be a focused beam for irradiation purposes even at the maximum momentum of the AD.

1 Introduction

For the so-called measurement line, DEM, at the Antiproton Decelerator (AD), the main constraints given in terms of optics are as follows:

- Good measurements of important properties of the AD beam such as transverse emittance and momentum spread at momenta between 100 MeV/c and 300 MeV/c
- Matching to the parameters for the Radio Frequency Quadrupole (RFQ) at the focus while preserving small beam sizes and large acceptances
- Availability of small and parallel beams for studies of antiproton channeling at 100 MeV/c
- Availability of a focused beam for irradiation purposes at 100 MeV/c, 300 MeV/c and 3.575 GeV/c

Apart from these constraints, there are of course the physical boundaries given by the shielding walls, the main beam lines for the experiments and the limited choice of available elements (quadrupoles and dipoles).

The calculations shown below are based on a transverse emittance of $\varepsilon = 5\pi$ mm·mrad, a momentum spread of $\Delta p/p = 10^{-3}$ and the values given correspond to $\pm 2\sigma$. The horizontal and vertical acceptances, defined as $A = \pi r_{\text{min}}^2/\beta_{\text{max}}$, are given in table 4 below.

2 RFQ matching

Since the deceleration of antiprotons with a Radio Frequency Quadrupole (RFQ) is technically demanding, it is necessary to be able to test the operation before installation in the DE1 line. There are several options for such a test, of which one is to use the measurement line.

As for the studies of the DE1 line where the RFQ is to be installed, it is important that the dispersion at the focus is zero, ie. that the dispersion invariant, $\varepsilon_D = \gamma D^2 + 2\alpha DD' + 2\beta D'^2$, after the last dipole must be as small as possible [1]. Here D denotes the dispersion, D' its derivative and α, β, γ the Twiss parameters. Furthermore, since the transverse emittance increase at a given position is proportional to β and the beam size proportional to $\sqrt{\beta}$, it is advantageous to keep the beam small during the transport. This also means that the influence of instability of the dipoles and quadrupoles on the Twiss parameters at the focal point is minimized. The values of these parameters are given by the construction of the RFQ [2]. Finally, the beam size at the position of the buncher, 6.15 m upstream of the focus, must be small.

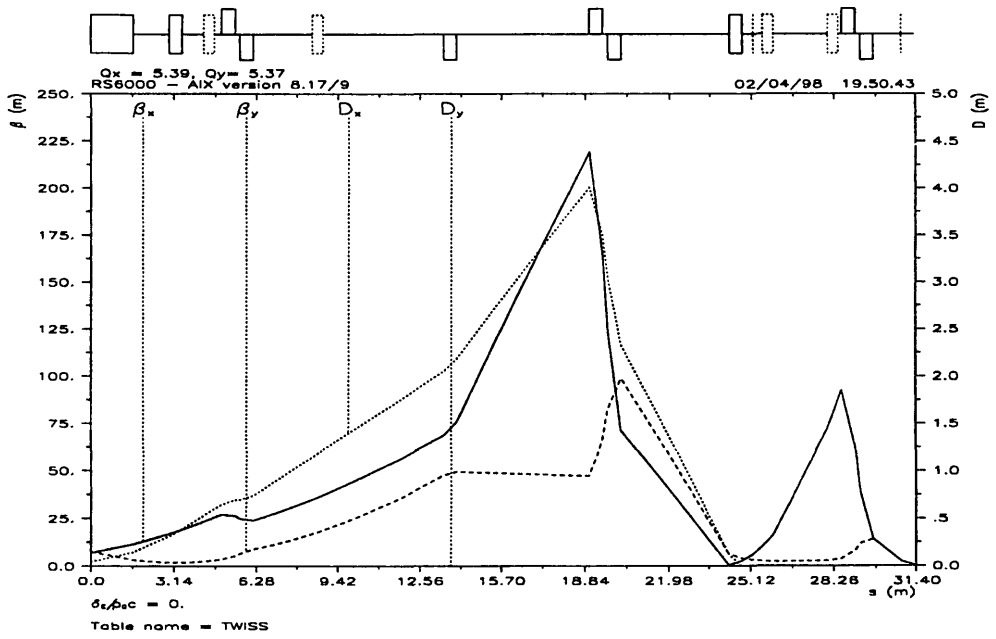

Figure 1: *Optical functions from the AD septum to the focal point of DEM for the test beam for the RFQ.*

In fig. 1 is shown the result of the matching performed to obey these constraints. Since this was expected to be the most difficult optimization, the position of the quadrupoles was defined by the need for a good match in this situation.

3 Beam property measurements

Two important parameters of the AD beam must be measured as precisely as possible in the DEM line: The transverse emittance and the momentum spread. Furthermore, it is desirable to be able to measure these parameters in the momentum range 100-300 MeV/c [1].

3.1 Transverse emittance

The transverse emittance is proposed to be measured by a variation of the 'standard method' [5] where the beam size is usually detected in three Multi Wire Proportional Chambers (MWPCs), positioned symmetrically around a beam waist. The expression in the case of a straight section with spacing l between the chambers becomes:

$$\varepsilon \simeq \frac{w_1^2}{l}\frac{w_2}{w_1}\sqrt{\frac{w_3}{w_1} - \frac{w_2^2}{w_1^2}} \tag{1}$$

where w_i denotes the width of the beam measured at chamber i and it is assumed that $w_3/w_1 \simeq 1$ due to the symmetry. However, to accommodate three MWPCs in the rather limited space along a straight section of the measurement line means that their separation will be exceedingly small for an accurate measurement. Instead, it is proposed to reduce the number of MWPCs to two, with one directly connected to the last quadrupole before the waist and the second at the point where the waist is calculated to be. Clearly, the assurance of symmetry given by the third chamber is then lost, but one can instead minimize the size of the beam on the second MWPC, which reestablishes the symmetry, although with slightly smaller accuracy. In this case eq. (1) applies with $w_3/w_1 \equiv 1$, ie.

$$\varepsilon \simeq \frac{w_1^2}{l}\alpha_w\sqrt{1-\alpha_w^2} \tag{2}$$

where $\alpha_w = w_2/w_1$ is the ratio of observed beam widths in the chambers 1 and 2. If this method is chosen, clearly one has to change the setting of the optics between the measurements of horizontal and vertical transverse emittance.

A small complication may arise from the fact that the beam may vary from shot to shot, and that the MWPC profiles, which are destructive measurements, only can be done one at a time. This also means that the measurement of the transverse emittance can not be done in one shot, but requires at least two shots in both transverse planes.

A variation of the above may be considered, where one uses the 'pepper-pot' method to establish the beam size at one point.

[1] The possibility of measuring at even higher momenta was prevented by the non-existence of a sufficiently small dipole magnet with the required integrated field, given the layout of the zone between the main lines and the machine.

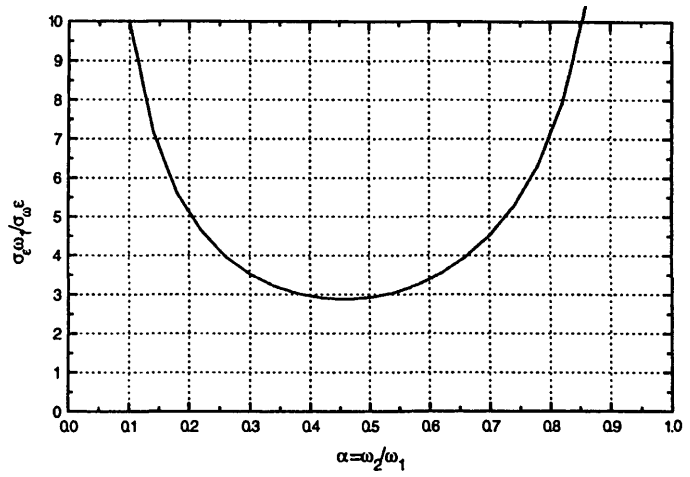

Figure 2: *The relative uncertainty, $\sigma_\varepsilon/\varepsilon$, of the transverse emittance as a function of $\alpha_w = w_2/w_1$ in units of σ_w/w_1 according to eq. (3).*

The RMS uncertainty in the determination of the transverse emittance, σ_ε, is given from the uncertainty of the widths, σ_{w_i}, obtained by the MWPCs by

$$\frac{\sigma_\varepsilon}{\varepsilon} \simeq \sqrt{(\frac{\sigma_l}{l})^2 + (\frac{\sigma_{w_1}}{w_1}(1 + \frac{\alpha_w^2}{1-\alpha_w^2}))^2 + (\frac{\sigma_{w_2}}{w_2}(1 - \frac{\alpha_w^2}{1-\alpha_w^2}))^2} \qquad (3)$$

However, the knowledge of the focal length l_f (ie. the assumption $w_3/w_1 \equiv 1$) hinges on the accuracy of the measurement of the widths, w_i, which each contribute $\sigma_{w_i}/w_i \cdot \alpha_w/(1-\alpha_w)$ to σ_l/l. The uncertainty in the determination of the distance between the MWPCs has been neglected.

In the case where $\sigma_{w_1} = \sigma_{w_2}$, the optimum value is $\alpha_w = 0.456$ which leads to $\sigma_\varepsilon/\varepsilon \simeq 2.88 \cdot \sigma_w/w_1$ and $\varepsilon \simeq 0.406 \cdot w_1^2/l$, according to eqs. (3) and (2). The relative uncertainty, $\sigma_\varepsilon/\varepsilon$, varies less than 3% in the interval $0.4 \leq \alpha_w \leq 0.5$, see figure 2. As $\sigma_{w_i} = w_i/\sqrt{2N}$ where N is the number of particles used for the determination of w_i (assumed Gaussian) and $N \simeq 10^7$ per shot, the *limiting* accuracy for the measurement of the transverse emittance becomes approximately $\sigma_\varepsilon/\varepsilon \simeq 6 \cdot 10^{-4}$.

An important and interesting feature of the ejected beam in the experimental lines and in the measurement line is the so-called 'effective overall emittance'. This is understood as the area of phase-space which includes a certain fraction of the beam, averaged over many shots. Due to random errors in quadrupoles, dipoles and septum, the effective overall emittance may be somewhat larger than the transverse emittance of the beam itself. Values around 10 π mm·mrad are not unrealistic during the initial phase of

the AD and since the RFQ has been designed with an acceptance of 15 π mm·mrad [2], it is desirable that (effective overall) emittances of this magnitude can be measured. On the other hand, a transverse emittance of around 1 π mm·mrad is expected to be a lower limit due to restgas scattering during the final flat top at 100 MeV/c before extraction [3]. This means that the emittance measurement, eq. (2), must cover a factor $\simeq$15. Furthermore, it might be useful to be able to measure the corresponding quantities at 300 MeV/c, which sets a lower limit on the focal length and therefore l in eq. (2). The upper limit is to a large extent imposed by the configuration of the line. The choice $l = 0.9$m with $\alpha_w = 0.456$ leads to $w_1[\text{mm}] = 1.49\sqrt{\varepsilon[\pi \text{ mm} \cdot \text{mrad}]}$, ie. $\beta = 2.22$ m, which means that a detector with 1 mm resolution and 16 channels is well suited for the purpose[2].

The above requirements can be fulfilled even with a horizontal dispersion and derivative of dispersion of essentially zero in the last part of the line. The result of the matchings are shown in figures 3 and 4, between which only the elements downstream of ATP.BHZ8000 are changed.

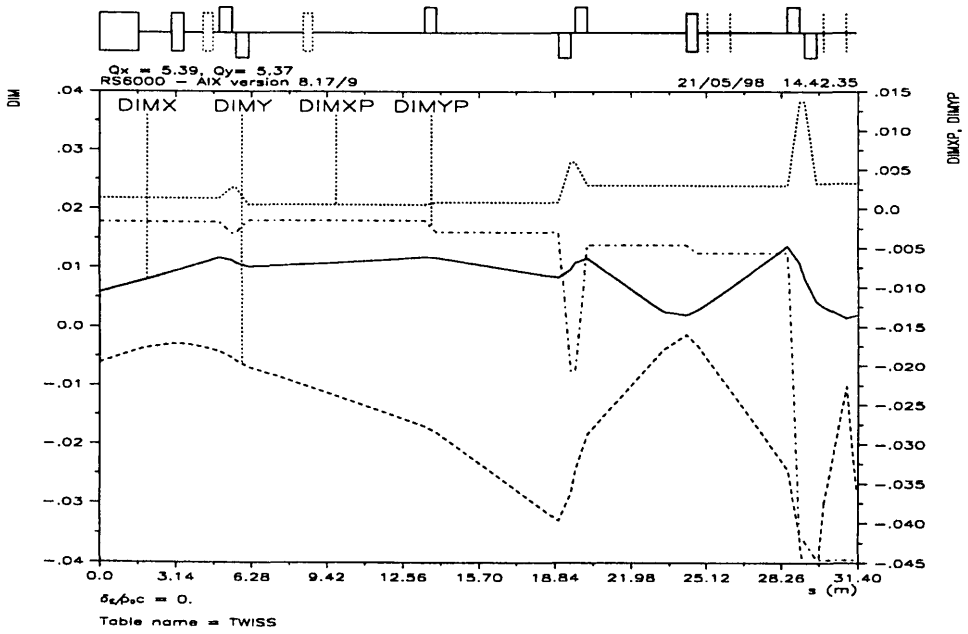

Figure 3: *Beam size and divergence from the AD septum to the focal point of DEM for the measurement of horizontal transverse emittance.*

[2]For a shot with 10^7 particles there will be a significant number of counts even at 6σ.

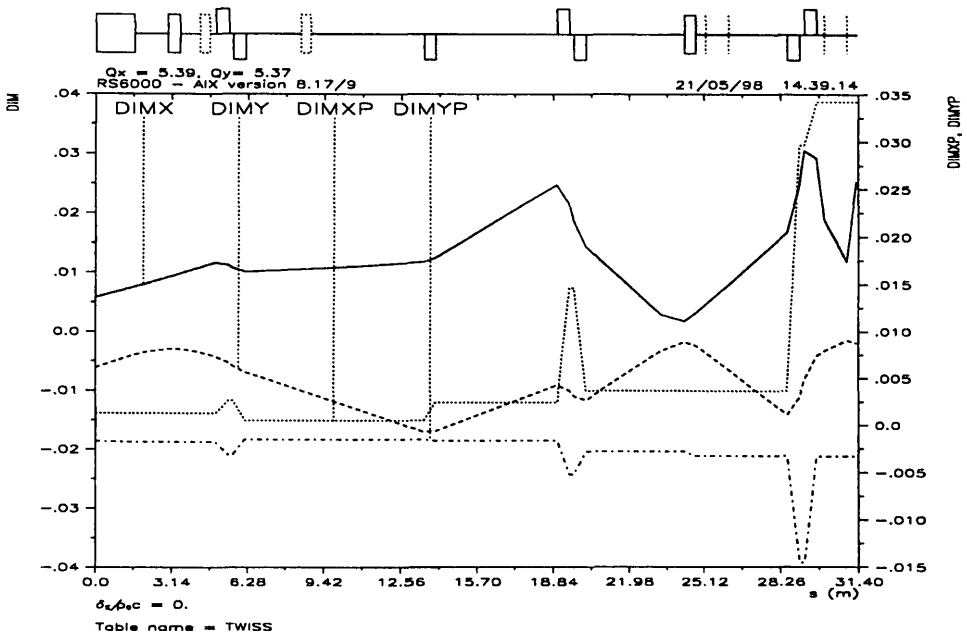

Figure 4: *Beam size and divergence from the AD septum to the focal point of DEM for the measurement of vertical transverse emittance.*

3.2 Momentum spread

The momentum spread is measured by increasing the dispersion invariant after the 30° deflection before the focus. The expected values are of the order 5π mm·mrad for the transverse emittance and a momentum spread, $\Delta p/p$, around 10^{-3} for the antiproton beam. Since the size of the beam is found as

$$x = \sqrt{\varepsilon\beta + D^2\frac{\Delta p^2}{p^2}} \leq \sqrt{\beta(\varepsilon + \varepsilon_D\frac{\Delta p^2}{p^2})} \tag{4}$$

the dispersion invariant must be more than 10^6 times larger than the transverse emittance, ie. $\varepsilon_D \gg 5\pi$ m·rad, to become the dominant factor that determines the size of the beam at a given location[3]. The values obtained at MWPC1 (upstream the 30° bend), MWPC2 and MWPC3 (downstream the 30° bend) are given in table 1 and the beta-function and dispersion is shown in figure 5. These values lead to expected sizes due to momentum spread and transverse emittance of 0 mm and 28 mm at MWPC1 and 7.9 mm and 3.3 mm at MWPC3, respectively, such that a comparison may lead to a determination of the momentum spread. This is under the assumption that β and D are known at both locations such that the MWPC1 measurement gives the transverse emittance which can be used to extract the momentum spread from the beam size ob-

[3]The maximum value for the dispersion becomes $D^{\max} = \sqrt{\beta\varepsilon_D}$, such that there is always a connection between the size of the beam and the maximum possible value of the dispersion.

served at MWPC3. These optical functions may be determined by use of the emittance measurement described above and the calibration procedure described below.

	D_x [m]	D_y [m]	$\varepsilon_{D,x}$ [m·rad]	$\varepsilon_{D,y}$ [m·rad]	β_x [m]	β_y [m]
MWPC1	0.0	0	0.32	0	156	78
MWPC2	4.34	0	28	0	1.05	155
MWPC3	7.89	0	28	0	2.19	251

Table 1: *Dispersion, dispersion invariant and beta-functions for the horizontal and vertical planes at the locations of three MWPCs.*

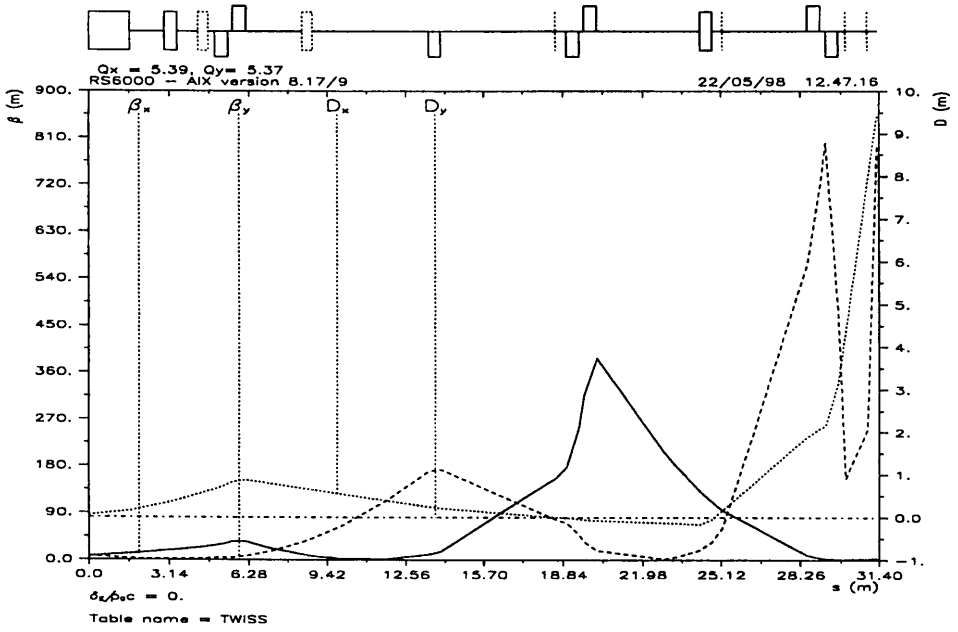

Figure 5: *Optical functions from the AD septum to the focal point of DEM for the optics for momentum spread measurements.*

To calibrate the line (measure the dispersion with given optics), one may use the relation between the variation of RF frequency and momentum, $\eta = p/f \cdot df/dp = 1/\gamma^2 - 1/\gamma_t^2$, where $\gamma_t = 4.750$ is the Lorentz factor at transition for the AD lattice and $1/\gamma_t^2 = \alpha = 0.0443 \simeq 1/Q_x^2$ the momentum compaction, with Q_x as the horizontal tune, ie. $\eta = 0.0201$ at 3.5752 GeV/c and $\eta = 0.944$ at 0.1 GeV/c. The momentum in the AD can be easily adjusted within $\pm 3\%$ of 0.1 GeV/c by use of the RF. Due to a dispersion of 4.4 cm at the extraction septum (and more in other proposed AD optics), one may not be able to extract more than $\pm 10^{-3}$ around the central momentum. This is, however, sufficient for the above purposes.

4 Beam for channeling

Following the succesful test of the feasibility of antiproton channeling [4], it has been proposed to study this phenomenon in more detail, also in view of possible use as a diagnostics device for instance at the AD.

Channeling is among other things characterized by the existence of a critical angle, the so-called Lindhard angle. A channeled beam must have a divergence at the point of the crystal which is smaller than or at least comparable to the critical angle which for singly charged particles at 100 MeV/c is of the order of 5 mrad for axial effects and roughly a third of that for planar effects, depending on the crystal material. At the same time as being parallel (ie. small $\sqrt{\varepsilon/\beta}$), the beam must maintain a size which maximizes the number of useful antiprotons on the limited surface available on a thin crystal (ie. small $\sqrt{\varepsilon\beta}$). As this evidently presents two competing requirements given the emittance, two beams were studied: One which is relatively parallel with a size of approximately 1 cm in diameter as expected for a thin crystal, and another which is very parallel at the expense of a large size at the focal point. The first is expected to be used for eg. a rough alignment of the crystal with the beam, while the latter can be used for the real measurement.

	x [mm]	y [mm]	x' [mrad]	y' [mrad]	$\beta_x^{\max}$ [m]	$\beta_y^{\max}$ [m]
Small, parallel beam	12	12	0.41	0.42	111	58
Large, parallel beam	45	45	0.12	0.12	401	736

Table 2: *Transverse dimensions, divergences and maximum values of the beta-function for the two beams studied for antiproton channeling.*

In both cases, the dispersion and its derivative at the focus is essentially zero.

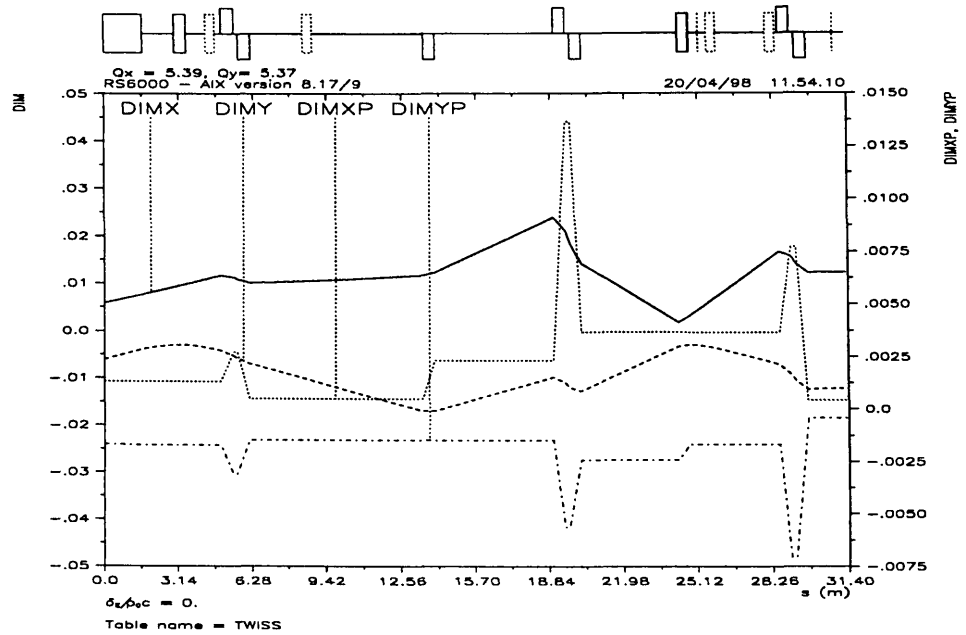

Figure 6: *Beam size and divergence from the AD septum to the focal point of DEM for the small and parallel beam for antiproton channeling.*

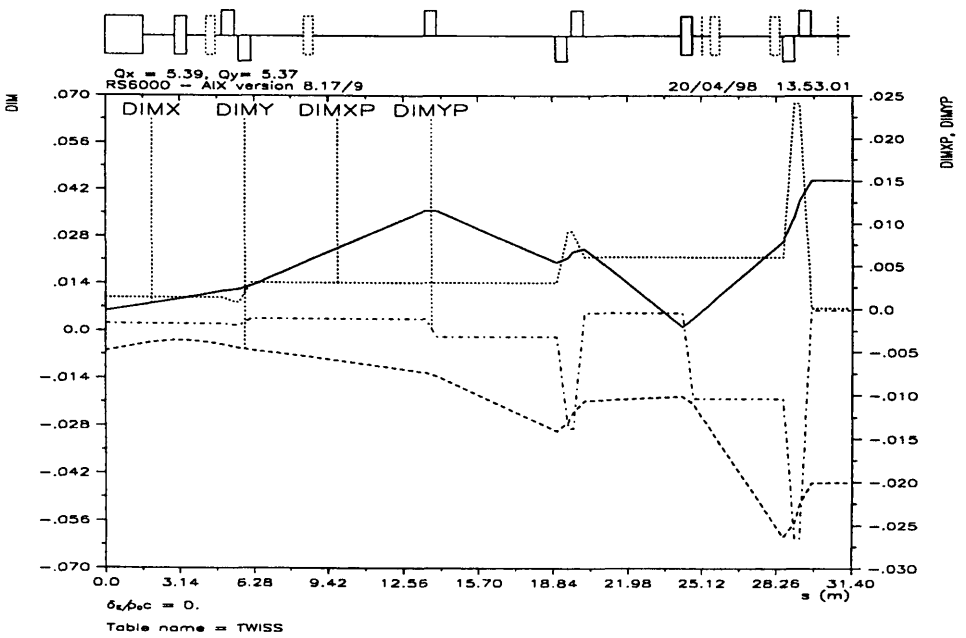

Figure 7: *Beam size and divergence from the AD septum to the focal point of DEM for the large and parallel beam for antiproton channeling.*

5 Beam for irradiation

For irradiation purposes, a focused beam must be available, preferably at both low and high momentum. Thus, three different optics were studied. For one low-momentum beam, the focal size is relatively small as is the maximum value of the beta-function in the transport. For the other, the focal size is reduced by approximately a factor of 3 at the expense of a somewhat larger maximum value of the beta-function in the transport. In both cases, the dispersion and its derivative at the focus is essentially zero.

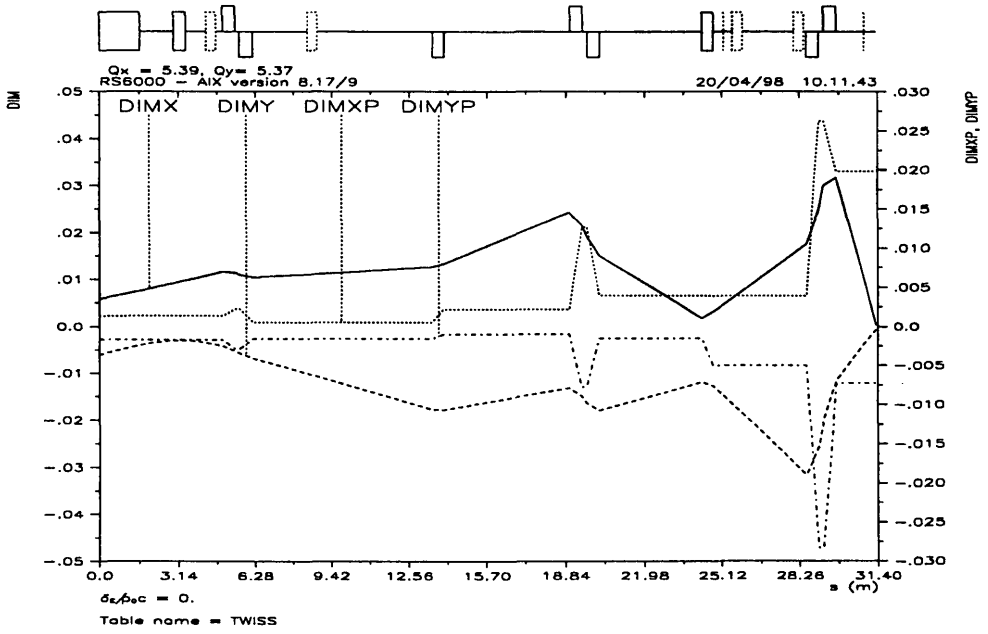

Figure 8: *Beam size and divergence from the AD septum to the focal point of DEM for the small and weakly focused beam for irradiation.*

To be able to irradiate at 3.575 GeV/c the section of vacuum upstream the last 30° bend may be reduced which will leave room for an irradiation zone of approximately 1×1 m^2. In this case, the dispersion at the focus can not be reduced to zero, due to the fact that the only deflection after the septum magnet is at the DE.BHZ 7010 upstream of which there are no elements available for tuning. Nevertheless, a focal size of approximately 2×1 mm^2 has been obtained, with a horizontal dispersion of 0.5 m. The values for the studied solution are given in table 3.

Finally, the question of radiation safety for this option has been discussed with TIS [6]. For the 3.6 GeV/c beam there has to be installed an additional beam stop, a beam dump along the wall which separates the DEM zone from the machine as well as sufficient shielding (according to the proposed setup) around the specimen to be irradiated. It

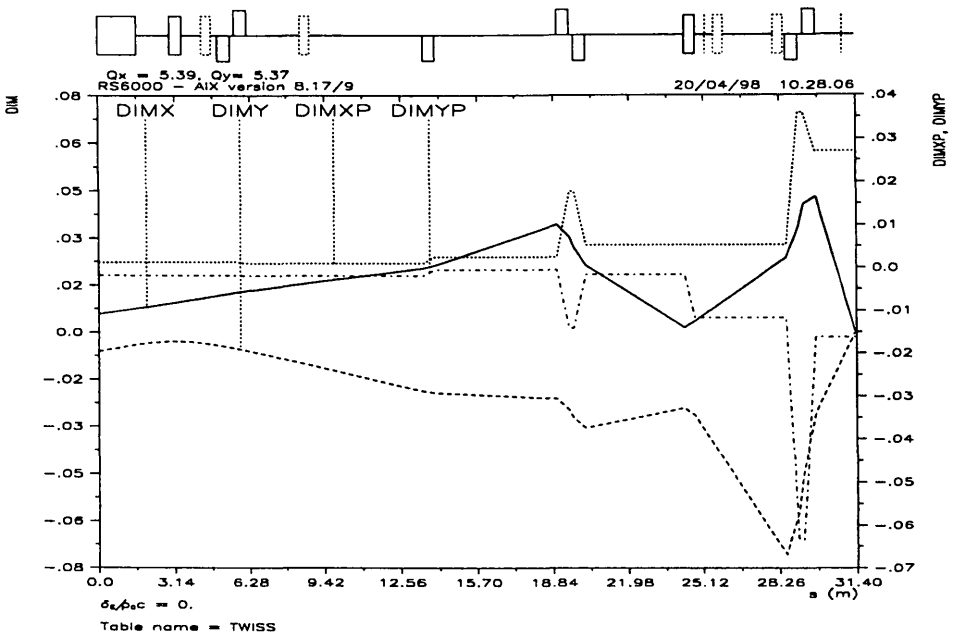

Figure 9: *Beam size and divergence from the AD septum to the focal point of* **DEM** *for the large and strongly focused beam for irradiation.*

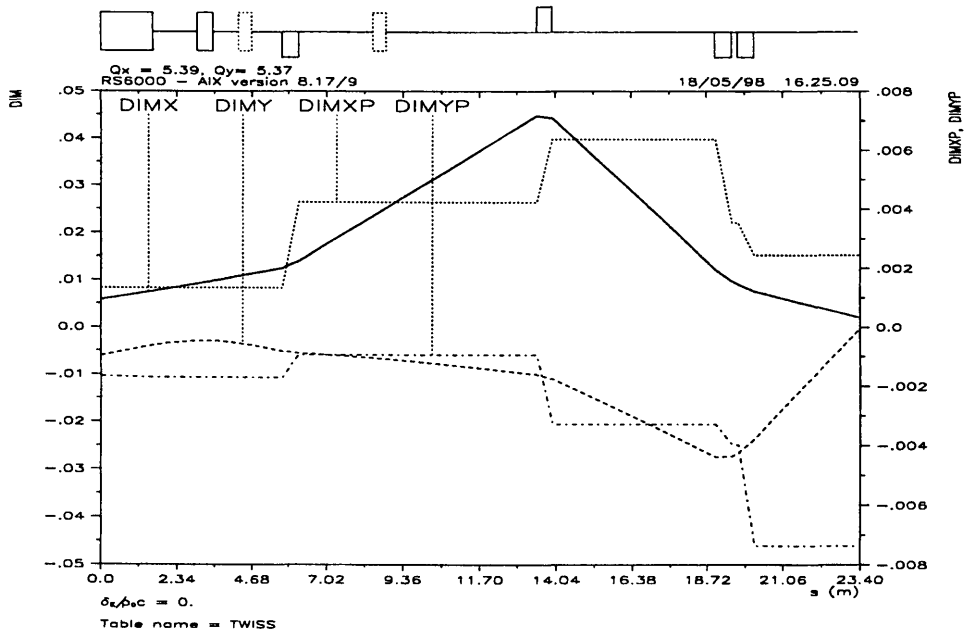

Figure 10: *Beam size and divergence from the AD septum to the 'reduced' focal point of* **DEM** *- upstream the 30° bend - for the 3.575 GeV/c beam for irradiation.*

	x [mm]	y [mm]	x' [mrad]	y' [mrad]	β_x^{max} [m]	β_y^{max} [m]
Small focus, 0.1 GeV/c	0.25	0.69	20	7.3	200	200
'Micro' focus, 0.1 GeV/c	0.19	0.31	27	16	370	1000
Small focus, 3.6 GeV/c	2.1	0.80	2.4	7.4	400	151

Table 3: *Transverse dimensions, divergences and maximum values of the beta-function for the three beams studied for irradiation purposes.*

is also a possibility to install a y-shaped vacuum chamber in the 30° bend and let the focal point be straight downstream of the bend. The radiation safety aspects have thus been superficially studied, but final approval must await a more specific arrangement, following a proposal for irradiation.

The change-over from normal 100-300 MeV/c operation to extraction of 3.6 GeV/c requires recabling of the ejection septum (to a different power supply), connection of the kicker in the AD section 35 as well as recabling of the bend and quadrupoles in the 7000 line. Switching between antiproton modes without intervention is thus not possible.

6 Conclusion

The layout and optics of the so-called measurement line at the AD have been studied and suitable solutions have been found to accomodate a variety of beam requirements, while relying on existing elements. The possibilities include:

1. Good measurements of important properties of the AD beam such as transverse emittance and momentum spread at momenta between 100 MeV/c and 300 MeV/c
2. Matching to the parameters for the RFQ at the focus while preserving small beam sizes and large acceptances
3. Small and parallel beams for studies of antiproton channeling at 100 MeV/c
4. Focused beams for irradiation purposes at 100 MeV/c, 300 MeV/c and 3.575 GeV/c.

The calculated acceptances, $A = \pi r_{\min}^2/\beta$, are given in table 4.

	A_x	A_y
RFQ (incl. buncher)	20	33
Measurement, ε	41	23
Measurement, $\Delta p/p$	5	16
Irradiation, small	39	25
Irradiation, 'micro'	17	7
Irradiation, 3.6 GeV/c	6	90
Channeling, small	43	38
Channeling, large	9	20

Table 4: *Acceptances, $A = \pi r_{\min}^2/\beta$, given in π mm·mrad for the optics studied.*

The layout of the DEM beam line and experimental area is shown in figure 11.

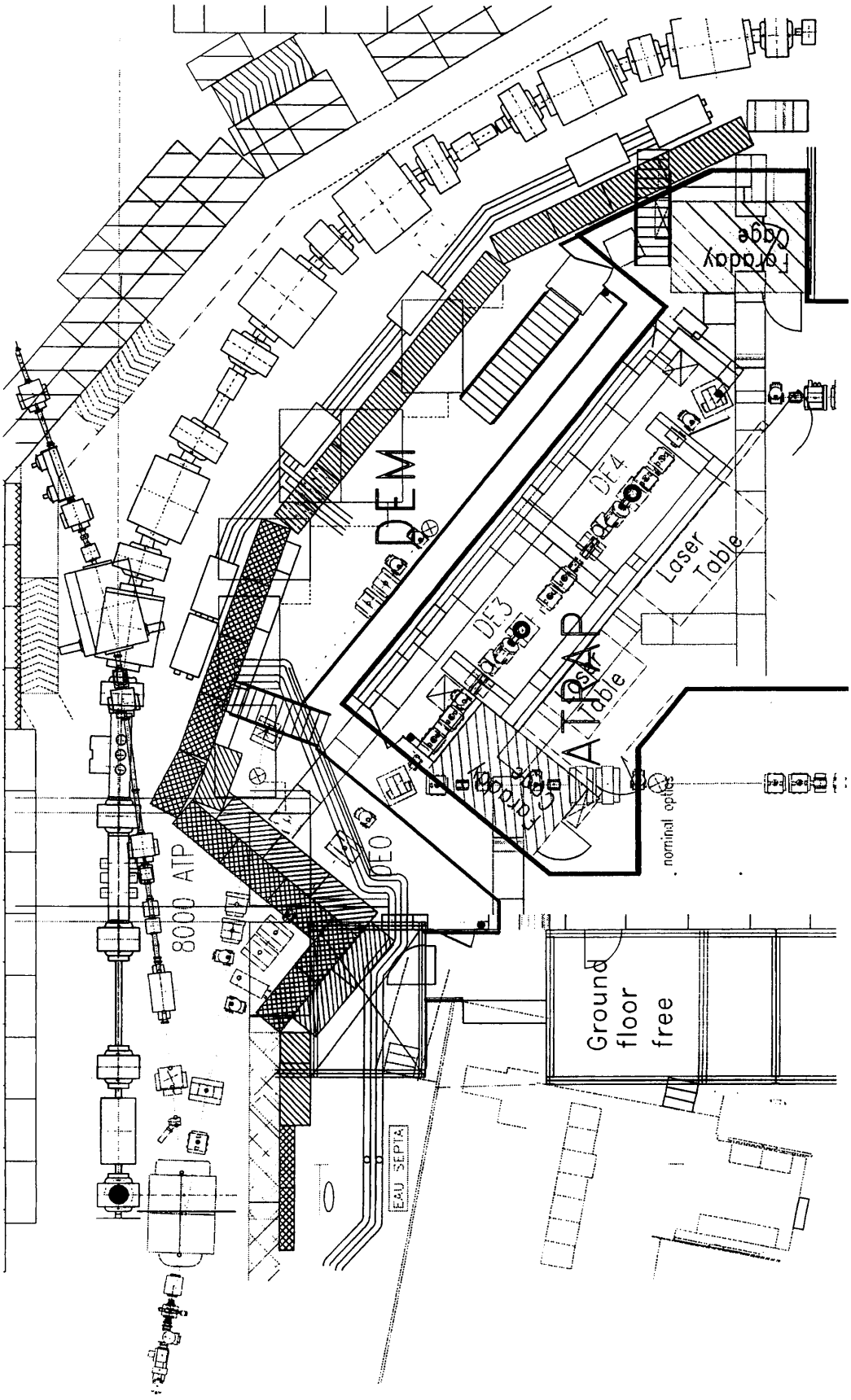

Figure 11: *Layout of the DEM beam line and experimental area.*

Mode	DEM.QN 10-1	DEM.QN 20-1	DEM.QN 30-1	DEM.QN 40-1	DE0.QN10	DE.Q 7020-1	DE.Q 7030-1
Chann. small	73.25425	-66.71615	72.75978	-64.34398	-0.540706	12.1470	-9.47375
Chann. large	-62.68713	65.61542	-65.14233	59.99669	0.551769	0.931922	-6.18532
RFQ	75.35699	-75.27132	123.06307	-145.92436	-0.280239	9.20475	-8.91843
Irrad. small	67.14071	-55.86993	-117.66088	149.4489	-0.446502	10.50338	-7.79090
Irrad. 'micro'	65.40731	-56.07343	-118.66186	150.06292	-0.248203	0.0	0.34400
Meas. D	-54.86233	62.30022	11.24312	-154.19493	-0.581269	-4.163659	15.02308
Meas. ε_h	-79.13768	82.2163	136.29287	-194.41357	0.279867	12.08489	-9.441785
Meas. ε_v	76.02281	-72.16568	-140.39022	207.96854	-0.567909	12.08489	-9.441785
Irrad. HE	-993.5857	-510.58296	-	-	7.18521	0.0	-298.4023

Table 5: *Currents given in A for the quadrupoles in the 7000,* `DE0` *and* `DEM` *line for the different optics studied. All currents are given for the case of 0.1 GeV/c, except the irradiation at high energy, Irrad. HE, given for 3.5752 GeV/c. It is thus possible to use all these optics also at 0.3 GeV/c, since the quadrupoles are approximately linear in gradient versus current up to the limit at* $\simeq$*1000 A.*

References

[1] U. Mikkelsen, PS/CA Note 98-08

[2] J. Bosser *et al.*, PS/HP Note 97-36

[3] N. Madsen, private communication

[4] S.P. Møller *et al.*, Phys. Rev. A **56**, 2930 (1997)

[5] M. Arruat and M. Martini, CERN/PS 92-59 (PA)

[6] D. Forkel-Wirth and A. Muller, TIS/RP, private communication, 1998

Distribution

P. Belochitskii
T. Eriksson
R. Giannini
M. Giovannozzi
J.-Y. Hémery
A. Lombardi
S. Maury
C. Metzger
D. Möhl
F. Pedersen
W. Pirkl
J.P. Riunaud
G. Segura Millan
T. Spickermann